



Published in final edited form as:

Carbon N Y. 2008 March ; 46(3): 489–500. doi:10.1016/j.carbon.2007.12.018.

Targeted Removal of Bioavailable Metal as a Detoxification Strategy for Carbon Nanotubes

Xinyuan Liu¹, Lin Guo², Daniel Morris², Agnes B. Kane³, and Robert H. Hurt^{2,*}

¹Department of Chemistry, Brown University, Providence, Rhode Island ²Division of Engineering, Brown University, Providence, Rhode Island ³Department of Pathology and Laboratory Medicine; Brown University, Providence, Rhode Island

Abstract

There is substantial evidence for toxicity and/or carcinogenicity upon inhalation of pure transition metals in fine particulate form. Carbon nanotube catalyst residues may trigger similar metal-mediated toxicity, but only if the metal is bioavailable and not fully encapsulated within fluid-protective carbon shells. Recent studies have documented the presence of bioavailable iron and nickel in a variety of commercial as-produced and vendor “purified” nanotubes, and the present article examines techniques to avoid or remove this bioavailable metal. First, data are presented on the mechanisms potentially responsible for free metal in “purified” samples, including kinetic limitations during metal dissolution, the re-deposition or adsorption of metal on nanotube outer surfaces, and carbon shell damage during last-step oxidation or one-pot purification. Optimized acid treatment protocols are presented for targeting the free metal, considering the effects of acid strength, composition, time, and conditions for post-treatment water washing. Finally, after optimized acid treatment, it is shown that the remaining, non-bioavailable (encapsulated) metal persists in a stable and biologically unavailable form up to two months in an *in vitro* biopersistence assay, suggesting that simple removal of bioavailable (free) metal is a promising strategy for reducing nanotube health risks.

1. Introduction

Most commercial carbon nanotube (CNT) samples contain ultrafine metal particles derived from the original growth catalyst or support. Over 20 metals have been used as CNT catalysts, but most commercial samples use formulations that incorporate Fe, Ni, Y, Co, and/or Mo. Many commercial carbon nanotube samples have been post-processed to reduce metal and/or amorphous carbon, and to increase the nanotube fraction, but even these “purified” samples typically contain significant quantities (1.2–14.3%) of residual metal [1,2]. Nanotube purification technologies continue to improve [3–9], but deep purification can damage tube structure [10–12] and for the foreseeable future, most CNT samples will contain metals.

Fine metal-containing particles pose known inhalation health risks [13–15], based on studies concerned with occupational health and safety in the metals industry [16,17] or the health effects of atmospheric fine and ultrafine particulates [18–20]. Based on these studies, and on the limited available literature on nanotube toxicity [21–28], there is a real concern that CNT-

*corresponding author, Robert Hurt, Robert_Hurt@brown.edu Tel: 401 863-2685, Fax: 401 863-9120.

Publisher's Disclaimer: This is a PDF file of an unedited manuscript that has been accepted for publication. As a service to our customers we are providing this early version of the manuscript. The manuscript will undergo copyediting, typesetting, and review of the resulting proof before it is published in its final citable form. Please note that during the production process errors may be discovered which could affect the content, and all legal disclaimers that apply to the journal pertain.

metals will trigger similar mechanisms of toxicity and carcinogenicity. To trigger these mechanisms, however, requires exposure of the metal surfaces to physiological fluid phases for biological surface reactions or release of soluble metal into those fluids. Dissolution and toxicant leaching are important phenomena influencing the biological responses to many types of fine particles and fibers [29]. Two recent studies examined the bioavailability of CNT iron [1] and nickel [2] by developing assays for the release of soluble metal ions into physiological model fluids and applying them to a range of nanotube samples and processing conditions.

A surprising result from those two studies was the existence of measurable bioavailable metal in each of the “purified” materials supplied by commercial vendors [1,2]. Figure 1 shows representative data from those studies, in which the commercial purification processes leave significant bioavailable metal (samples A, B) or even *increase* bioavailable metal (sample C). Metal removal steps typically involve acid washing, and the portion not removed is commonly assumed to be encapsulated within carbon shells and would not be expected to be released during a bioavailability assay. It is not obvious how acid washing leaves unencapsulated (bioavailable) metal as implied by Fig. 1. Understanding the origin of bioavailable metal in “purified” samples is an important first step in the development of purification processes designed for detoxification.

The present study addresses several questions unanswered by these previous studies:

1. What is the origin of bioavailable metal in “purified” samples?
2. How can purification processes be modified to improve the removal of the bioavailable metal fraction?
3. If techniques can be developed to remove bioavailable metal, will the remaining, encapsulated (non-bioavailable) metal be stable during longer-term exposure to physiological fluids or cells following human exposure?

This last question relates to the biopersistence of the carbon shell structures, and is important for understanding whether the concept of bioavailable metal removal is *sufficient* as a practical detoxification strategy, or if *all* metal must be removed in order to avoid metal-induced toxicity.

This paper addresses these three questions focusing on nickel and iron in a set of commercial SWCNTs. We note that some of the samples also contain yttrium, and our preliminary data indicate that Y is mobilized into solution in a manner similar to Ni and Fe. However, preliminary cell toxicity studies in our laboratories suggest low toxicity for mobilized Y, so we choose to focus on Fe and Ni, which are well established pulmonary toxicants [30]. There is strong motivation to manage nanotube metal release, and the results presented here provide practical guidance for intelligent post-processing to reduce carbon nanotube health risks and enable safe commercialization.

2. Materials and Experimental Procedure

2.1 Materials

Seven samples of single-wall carbon nanotubes were purchased from different commercial vendors. As seen in Table 1, these samples have significant and widely varying metal contents including the “purified” materials supplied by most vendors. Additional data showing the range of metals contents in commercial CNTs is given in our previous articles on metal bioavailability [1,2]. A sample of typical morphologies in as-produced SWCNTs are shown in Fig. 2, which show mixtures of SWCNT bundles, amorphous carbon, graphitic nanoshells and metal nanoparticles that are dark under TEM. Vendor purified SWCNTs show a variety of carbon shell types (empty, metal filled, partially filled), which may imply varying defect densities that determine the shell fluid protective properties [1,2].

Ni nanoparticles of nominal particle size 15–25 nm were purchased from Alfa Aesar (Ward Hill, MA). NiO nanoparticles were prepared by heating the commercial Ni nanoparticles in a TA Instrument 951 thermogravimetric analyzer (TGA) at 10°C/min followed by a 60 min isothermal hold at 775°C. TGA residues were characterized on a Bruker AXS D8 Advance X-ray Diffractometer (XRD) and the all the 5 peaks on the diffraction pattern can be readily indexed as crystalline NiO (JCPDS 47-1049) (111), (200), (220), (311) and (222) respectively (data not shown).

Nickel(II) chloride hexahydrate, iron(II) sulfate heptahydrate, sodium L-ascorbate, 2-deoxy-D-ribose, 2-thiobarbituric acid and trichloroacetic acid were purchased from Sigma Aldrich Chemical Co. (St Louis, MO) and ferrozine from Aldrich Chemical (Milwaukee, WI). Iron (III) chloride hexahydrate was purchased from Alfa Aesar Company (Ward Hill, MA).

In this study we use phagolysosomal simulant fluid (PSF) described by Stafaniak et al [32], which is designed to mimic the chemical environment within phagolysosomes, the intracellular compartment in which nanomaterials are localized following their internalization by phagocytosis (Table 2). At the low pH inside lysosomes, we expect the highest dissolution rates for metal nanoparticles [2].

2.2 Methods

2.2.1 Metal mobilization (bioavailability) assays—Nickel mobilization was measured by the following procedure: single-wall nanotube suspensions (1.0 mg/ml) were incubated in various aqueous solutions (DI H₂O at pH 7.0, acetate buffer at pH 5.5 or 4.5, or PSF at pH 4.5) by ultrasonication in a Branson 5510 ultrasonic water bath for 2 hr followed by centrifugal ultrafiltration (5000 NMWL Amico centrifugal filter devices, Millipore, MA) on a Jouan CT422 centrifuge (4000rpm, 0.5–1hr) to remove the carbon nanotubes and any free Ni nanoparticles. The clear nickel ion containing solutions free of any solid particulates were collected in the bottom and analyzed by a Jobin Yvon JY2000 Ultrace inductively coupled plasma atomic emission spectrometer. Measurements were made at a wavelength of 221.647 nm and intensities were calibrated using six standards ranging in concentration from 0 to 5 ppm or 0 to 100 ppb depending on the concentration range.

Iron bioavailability was measured by a similar procedure: nanotubes were mixed with buffer solutions (PSF at pH 4.5 or phosphate buffered saline (PBS) at pH 7.4) at a concentration of 1.0 mg/ml. In some experiments, the Fe²⁺-chelator ferrozine and the reductant sodium L-ascorbate were added at 1 mM, and the mixtures were sonicated in an ultrasonic water bath for 2 hours followed by centrifugal ultrafiltration. The Fe-content of the CNT-free filtrates was also determined by ICP.

2.2.2 Ion adsorption experiments—To determine if soluble metal ions can adsorb on CNT outer surfaces during or after acid washing, nanotubes or reference carbon materials were added to metal ion solutions (FeCl₃, NiCl₂, FeSO₄ or CaCl₂ in either D. I. water or 3M HCl) at concentrations between 0.1 to 1 mg/ml and ultrasonicated for 1–2 hours. After sitting at room temperature from 8 to 24 hrs, the solid particulates were removed by centrifugal ultrafiltration and the filtrate was analyzed for Fe, Ni, or Ca by ICP.

2.2.3 Acid washing experiments—To target the bioavailable metal, non-oxidizing acids were used to attack the fluid-accessible metal without damaging the carbon shells and potentially exposing fresh metal surface. In the search for an optimal treatment protocol, a variety of times, acid components, concentrations, and post-treatment water wash conditions were explored. The basic experiments involved one or more primary washes with 3 M HCl in 15 ml centrifuge tubes containing 0.1–1.5 mg CNT/ml, followed by ultrasonication, and incubation at room temperature for 24 hrs either with or without mechanical shaking. The

nanotubes were then removed by centrifugal ultrafiltration as above and subjected to one or more hot or cold water washes (10–40 ml per wash) followed by transfer to clean, dry 20-mL glass vials and overnight drying at 100 C. In some cases the acid concentration was reduced gradually in a series of washes from 3M, to 1, 0.3, or 0.1 M before the pure water wash steps. Selected experiments also used glacial acetic acid in the primary acid washing step.

2.2.4 Flow-through assay for longer-term stability (biopersistence) of carbon-coated metal—To test the longer term stability of encapsulated metal in our treated samples, a continuous flow-through assay was developed using a fluid medium designed to mimic the intracellular phagolysosomal environments. The covering carbon shells are key to the stability of the metal, and carbon is insoluble in buffer solutions even at low pH. We propose that the most plausible mechanism for physiological carbon attack and shell damage is *oxidation* (not acid dissolution). Phagocytic cells generate reactive oxygen species (ROS) by the enzyme NADPH oxidase or Phox triggering a respiratory burst [33]. Macrophages also sequester and actively pump iron into late endosomes and phagolysosomes where additional ROS are generated in order to kill phagocytosed microorganisms [34]. Phagocytosis of inert particulates, including ultrafine air pollutants, has also been shown to trigger the respiratory burst in lung macrophage [15]. To mimic this environment, we chose PSF at pH 4.5 augmented by continuous ROS generation driven by Fenton chemistry [35] using a custom dynamic flow-through assay [36].

Figure 3 shows the flow apparatus based on that of Scholze et al [37] but adapted for nanotubes and continuous ROS generation. To prevent loss of the ultrafine carbon nanotubes through filters, a nanotube mat is placed in a small shallow glass dish (5ml) and covered by glass wool. The combined CNT/glass fiber mat is held down gravitationally by glass beads and the test solution added drop-wise to the surface. The overflow passes through a fritted silica filter and is continuously collected and analyzed for Ni as an indication of carbon shell damage and Ni dissolution.

ROS are generated *in situ* by mixing 2X PSF containing 2mM H₂O₂ with 2mM ascorbate and 0.2mM FeSO₄ just above the sample vial. The individual solutions are delivered by peristaltic pumps (30ml/pump/day) from fresh stock solutions replaced daily (see Fig. 3).

The desired free radical generation was achieved by mixing physiologically relevant concentrations of iron, ascorbate, and hydrogen peroxide. The assay was validated by confirming ROS production in a static assay adapted from Lay et al [38,39]. In this assay, the pentose sugar, 2-deoxy-D-ribose, reacts with ROS to yield a mixture of products, which upon heating are converted to malondialdehyde (MDA) that reacts with 2-thiobarbituric acid (TBA) at low pH to form a pink chromophore quantifiable by absorbance at 532 nm. PSF solutions containing 1 mM H₂O₂, 1 mM ascorbate, 1 mM 2-deoxyribose and 0.1 mM FeSO₄ were vortexed for 5 seconds, and then incubated at 37°C for 2, 24 or 48 hr with continuous shaking. At the end of the incubation, the solution was centrifuged at 10,000 g for 10 min. Each sample was prepared in triplicate. A series of standard solutions was prepared by diluting a concentrated tetraethoxypropane (TMOP) [a.k.a. MDA bis(dimethyl acetal)] solution with PSF. To determine the MDA concentration in the samples, 1.0 ml of each supernatant or 1.0 standard solution was incubated with 1.0 ml 1.0% wt/vol (10mg/ml) TBA and 1.0 ml 2.8% wt/vol (28mg/ml) trichloroacetic acid (TCA) for 10 min at 100°C and then cooled on ice to stop the reaction. Absorbance at 532 nm was determined by spectrophotometry.

A final validation assay was carried out on the flow apparatus itself to ensure that the continuously generated ROS are not quenched by the glass beads or glass fiber filter. The full experiment was carried out without CNT addition and the overflow collected and incubated

with deoxyribose for 2 hr. The TBA assay produced pink color, indicating successful generation and survival of free radicals within the complete flow apparatus.

3. Results and Discussion

3.1 Measurement, origin, and removal of bioavailable nickel

3.1.1 Assay development for Ni bioavailability—Our previous work [2] used simple buffers to examine the effects of pH on nickel mobilization. Here we evaluate more complex media including the phagolysosomal simulant fluid (PSF) of Stefaniak et al. [32], which is designed to mimic the pH and ionic environment within intracellular phagolysosomes (see Materials) with the addition of reductants or oxidants. Figure 4 compares the Ni mobilization in PSF with that in simple buffer solutions and examines the role of the reductant ascorbate and the oxidant, H₂O₂. Based on these results, PSF at pH 4.5 was adopted as the standard solution for bioavailability assays in this study. For iron experiments the PSF is augmented by ferrozine and ascorbate (see section on Fe below), while for Ni it is used without augmentation.

3.1.2 Origin of bioavailable metal in vendor purified samples—A surprising result from our previous studies is detection of bioavailable (free) metal in each of the “purified” samples from commercial sources [1,2]. An important step toward decreasing metal-induced toxicity assorted with exposure to nanotubes is to identify the origin of this bioavailable metal, which should in principle have been removed by acid washing. We hypothesize contributions from several mechanisms:

- a. Kinetic limitations on acid dissolution combined with insufficient treatment time
- b. Redeposition of metal on CNT surfaces or functional groups
- c. Oxidative attack on protective carbon shells after or during acid purification.

Figure 5 provides insight into the role of kinetic limitations during acid washing. The partially etched metal observed inside some carbon shells indicates an ongoing dissolution process and can be expected to be a source of additional metal released in bioavailability assays. Nickel and nickel oxide in particular can be slow to dissolve in acid media, even when accessible. To test the intrinsic corrosion rates of these phases, we carried out acid washing experiments (3M HCl for 24 hr) on pure metallic Ni and NiO nanoparticles in the absence of carbon coating. This treatment mobilized 71% of the metallic Ni into solution, but only 9% of the Ni from in the NiO nanoparticles. Despite the nanoscale dimension of these particles, intrinsic corrosion rates can still limit their removal and the presence of NiO as a minority phase may make this removal even more difficult.

Figure 6 provides evidence for the second mechanism— re-deposition of soluble Ni on the free surfaces of nanotubes coupled with insufficient water washing. The adsorption data show the potential for CNTs to adsorb significant quantities of divalent cations, especially on carboxylic functional groups, while panel (c) shows that insufficient water washing can lead to detectable residual bioavailable Ni. Because nanotubes are often treated with oxidizing acids such as HNO₃ or H₂SO₄, carboxylic and other oxygen-containing functional groups are expected to be common at this stage of processing.

Figure 7 provides evidence for the third mechanism – that oxidation during or after acid dissolution can attack carbon shells and expose fresh metal without sufficient time for its removal by etching. Air oxidation can sharply increase bioavailable metal (panel a) by attack on carbon shells (See Liu et al. [2]). Simultaneous oxidation and acid washing as in “one-pot” purification processes tend to reduce total metal, but leave higher residual bioavailable metal than simple acid washing alone (panel b). We believe the difference is due to the continuous oxidation of carbon shells, which exposes fresh metal on an ongoing basis. At the end of the

treatment time, some metal has been only recently exposed and has not had time for complete removal by acid etching. Simple treatment with non-oxidizing acids or two-step oxidation and acid treatment are preferable to one-pot method to avoid late-stage damage to the covering carbon shells.

Based on these results we suggest that the bioavailable metal in purified samples is due to some combination of all three mechanisms, depending on the purification processing conditions.

3.1.3 Optimal removal by acid treatment—Figure 8 shows the effect of treatment time on the removal of bioavailable Ni by 3M HCl washing at room temperature. In the as-produced sample, bioavailable Ni is only gradually removed over 24 hrs. The vendor-purified sample behaves differently, with half of the initial metal mobilized by only 1 hr acid treatment, suggesting it may be in an easily accessible location on outer surfaces or bound to surface functional groups. Note that this particular commercial sample has the lowest bioavailable Ni in any of our studies (0.24 $\mu\text{g/ml}$), and it is reasonable to imagine that this small amount could represent re-deposited material.

Figure 9 shows the effect of acid composition removal of bioavailable Ni for four commercial samples at room temperature. Although there are reports of higher effectiveness with mixed acids containing acetic acid [40], there is no apparent benefit of this strategy in this data set. Overall, the use of 24 hr treatment in 3M HCl followed by three rounds of hot water washing is a near-optimal treatment, at least for room-temperature processing.

3.2 Measurement, origin, and removal of bioavailable iron

Avoidance and removal of bioavailable Fe poses many of the same issues as for Ni above. Figure 10 shows the comparison of different aqueous media as candidate simulant fluids for measuring bioavailable Fe. Similar to Ni, phagolysosomal simulant fluid at pH 4.5 is most effective at mobilizing soluble iron, but unlike Ni, ascorbate aids mobilization as does the Fe^{2+} -chelator, ferrozine. It is likely that ascorbate prevents oxidation to Fe^{3+} , and the formation of insoluble hydroxides and surface redeposition [41]. This idea is supported by the fact that ferrozine alone mobilizes Fe at the lower pH, where the Fe^{2+} to Fe^{3+} kinetics are known to be slower [42, 43]. Based on these results, PSF with ferrozine plus ascorbate was chosen as the standard for iron bioavailability assays for this study. Both ferrozine (Fe^{2+} chelator) and ascorbate (physiological reductant) increase iron mobilization and are recommended for determination of total bioavailable iron.

Figure 11 provides evidence that SWCNTs also adsorb soluble iron from solution. The adsorption is greatest for the carboxylic functionalized tubes, but is also significant for as-prepared tubes and for activated carbon as a high-surface-area reference material. Oxygen containing surface functional groups are likely sites for cation adsorption [44, 45].

Figure 12 explores the effect of wash medium composition on the removal of bioavailable iron from SWCNTs. The behavior of the as-produced material is similar to that for Ni removal, except that ascorbate addition improves removal. In contrast, the vendor-purified sample has bioavailable Fe that can be removed by simple water washing, and is bound either as a salt film or weakly adsorbed ionic species. The ease of removal of this residual bioavailable Fe is also seen in Figure 13, which examines the effects of acid/SWCNT ratio and time. Overall, the process of bioavailable Fe removal is a kinetically limited acid dissolution process for the as-produced material, but for this vendor purified sample it is the simple removal of weakly bound metal that was mostly likely re-deposited during washing at near neutral pH or drying. This iron is readily bioavailable and would likely be rapidly mobilized in the lungs following inhalation where it may catalyze ROS production and oxidant stress leading to lung injury [30].

3.3 Biopersistence of carbon shells and stability of encapsulated metal

The combined results presented up to this point show that bioavailable Ni and Fe in CNTs can be reliably reduced below 0.5 $\mu\text{g}/\text{ml}$ by careful acid treatment, water washing, and the avoidance of oxidation during or after the last stage of wet chemistry. In most cases, these processes will leave behind significant *non-bioavailable* (encapsulated) metal, and it is an open question whether that metal may be mobilized through long-term degradation processes in the lungs following inhalation exposure.

It is clear that the nanoscale metal residues in CNTs can be slowly dissolved if they are fluid accessible, so the key question is the physiological stability of the elemental carbon shells or tube walls that prevent this fluid access. Carbon materials are generally thought to be stable, or biopersistent, but little or no actual data are available on the long-term stability of nanotubes in physiologically-relevant environments. Elemental carbon cannot be dissolved in non-oxidizing weak acids, so we hypothesize that the most likely degradation mechanism would be *oxidation*. Some cellular compartments contain strong oxidants, including reactive oxygen species produced by the respiratory burst mechanism triggered by phagocytosis in alveolar macrophages [15]. In these target cells, continuous ROS generation driven by iron catalyzed redox cycling in late endosomes and phagolysosomes attack inert particulates or microorganisms [33].

Our approach is to simulate this intracellular environment with physiologically relevant concentrations of hydrogen peroxide, iron, and ascorbate [35], in order to assess the potential for gradual oxidative degradation of carbon shells and release of metal (see Fig. 14). To maintain this reactive fluid environment over time, we developed a flow-through assay (see Methods and Fig. 3) and applied it to one batch of the treated sample C-VP SWCNT for over a time course of two months. This batch of the SWCNT sample had the lowest bioavailable metal of any commercial sample studied to date (0.24 $\mu\text{g}/\text{ml}$) that was pre-reduced further in our laboratory by 3M HCl washing to about 0.08 $\mu\text{g}/\text{ml}$. (Note that the stability assay uses iron salts as a reagent, so it is only possible to apply the flow-through assay to the stability of carbon-encapsulated *nickel*.)

Figure 15 shows the results of the two-month assay. After an initial release of traces of Ni (< 0.04 $\mu\text{g}/\text{ml}$ in effluent), there is no further detectable release over the two month period, implying no significant damage to the fluid protective carbon shells. TEM analysis of the recovered purified VP SWCNTs also did not show any apparent carbon shell damage or any significant difference from the original sample before the flow-through assay. This is not entirely surprising, as the physiological oxidizing environment is much less harsh than chemical oxidizing environments used to functionalize carbon surfaces or remove amorphous carbon impurities. For example, the “one-pot” purification method described by Wang et al. [9] and used to generate Fig. 7 employs 30% H_2O_2 v/v, which is 9.7M or approximately 10^4 more concentrated than the 1 mM H_2O_2 solution used to simulate the phagolysosomal environment.

4. Conclusions

This study provides useful guidance for the proper measurement, avoidance, and removal of bioavailable metal in carbon nanotubes as a potential strategy for reducing their health risks. First, it was shown that a simple phagolysosomal simulant fluid at pH 4.5 is suitable for measuring bioavailable metal, though even simple acetate buffer at the same pH gives similar results. The fluid should be supplemented by ascorbate and ferrozine for determination of Fe release, which are not required in the assay for Ni release. These assays are easy to perform, reproducible, and are proposed as a quality control measure for CNT purification and processing. Second, the study provides guidance to improve current purification processes so

they do not leave residual bioavailable metal. Kinetic limitations on acid dissolution and insufficient treatment time, re-deposition on CNT outer surfaces or functional groups, and the use of oxidation steps during or after the final wet chemical treatment all can contribute to residual bioavailable metal in improperly purified materials. Third, treatment with a non-oxidizing strong acid (3M HCl) followed by multiple hot water washing as a *final* processing step is found to be a suitable method for targeted removal of bioavailable metal to levels below 0.5 µg/ml. The non-bioavailable (encapsulated) metal remaining after this treatment is found to be stable under simulated physiological conditions for up to two months. These results suggest that targeted removal of the bioavailable metal fraction is a promising strategy for minimizing CNT health risks. Finally, we note that metal effects are not the only toxicity mechanisms hypothesized for carbon nanotubes, and more work is needed to assess health risk that may be associated even with high purity tubes. For the impure materials that are now common in the marketplace, however, metal induced health effects are a real concern, and we suggest that these concerns can be adequately addressed by the targeted purification methods outlined here.

Acknowledgements

Financial support was provided by the NIEHS Superfund Basic Research Program P42 ES013660, EPA STAR Grant RD-83171901-0, NIEHS R01 ES016178, and NSF Nanoscale Interdisciplinary Research Team (NIRT) grant DMI0506661. Although this research was funded in part by the EPA and NIEHS, it does not necessarily reflect the views of either agency. The technical contributions of David Murray, Joseph Orchardo, William Turnbull, Charles Vaslet, Anthony McCormick and Indrek Kulaots at Brown University are gratefully acknowledged.

References

1. Guo L, Morris DG, Liu X, Vaslet C, Hurt RH, Kane AB. Iron bioavailability and redox activity in diverse carbon nanotube samples. *Chem Mater* 2007;19(14):3472–3478.
2. Liu X, Gurel V, Morris D, Murray D, Zhitkovich A, Kane AB, Hurt RH. Bioavailability of nickel in single-wall carbon nanotubes. *Adv Mater* 2007;19(19):2790–2796.
3. Shelimov KB, Esenaliev RO, Rinzler AG, Huffman CB, Smalley RE. Purification of single-wall carbon nanotubes by ultrasonically assisted filtration. *Chem Phys Lett* 1998;282:429–434.
4. Xu Y, Peng H, Hauge RH, Smalley RE. Controlled multistep purification of single-walled carbon nanotubes. *Nano Lett* 2005;5(1):163–168. [PubMed: 15792432]
5. Mathur RB, Seth S, Lal C, Rao R, Singh BP, Dhama TL, Rao AM. Co-synthesis, purification and characterization of single- and multi-walled carbon nanotubes using the electric arc method. *Carbon* 2007;45(1):132–140.
6. Fan H, Liu C, Liu C, Li F, Liu M, Cheng H. Purification of single-wall carbon Nanotubes by electrochemical oxidation. *Chem Mater* 2004;16(26):5744–5750.
7. Harutyunyan AR, Pradhan BK, Chang J, Chen G, Eklund PC. Purification of single-wall carbon nanotubes by selective microwave heating of catalyst particles. *J Phys Chem B* 2002;106(34):8671–8675.
8. Park T, Banerjee S, Hemraj-Benny T, Wong SS. Purification strategies and purity visualization techniques for single-walled carbon nanotubes. *J Mater Chem* 2006;16:141–154.
9. Wang Y, Shan H, Hauge RH, Pasquali M, Smalley RE. A highly selective, one-pot purification method for single-walled carbon nanotubes. *J Phys Chem B* 2007;111(6):1247–1252.
10. Dillon AC, Gennett T, Jones KM, Alleman JL, Parilla PA, Heben MJ. A simple and complete purification of single-walled carbon nanotube materials. *Adv Mater* 1999;11(16):1354–1358.
11. Hu H, Zhao B, Itkis ME, Haddon RC. Nitric acid purification of single-walled carbon nanotubes. *J Phys Chem B* 2003;107(50):13838–13842.
12. Martínez MT, Callejas MA, Benito AM, Cochet M, Seeger T, Ansón A, et al. Sensitivity of single wall carbon nanotubes to oxidative processing: structural modification, intercalation and functionalisation. *Carbon* 2003;41(12):2247–2256.

13. Serita F, Kyono H, Seki Y. Pulmonary clearance and lesions in rats after a single inhalation of ultrafine metallic nickel at dose levels comparable to the threshold limit value. *Ind Health* 1999;37(4):353–363. [PubMed: 10547950]
14. Zhang Q, Kusaka Y, Zhu X, Sato K, Mo Y, Kluz T, Donaldson K. Comparative toxicity of standard nickel and ultrafine nickel in lung after intratracheal instillation. *J Occup Health* 2003;45(1):23–30. [PubMed: 14605425]
15. Tao F, Gonzalez-Flecha B, Kobzik L. Reactive oxygen species in pulmonary inflammation by ambient particulates. *Free Rad Biol & Med* 2003;35(4):327–340. [PubMed: 12899936]
16. check the reference SnowETCostaMRomWNNickel toxicity and carcinogenesis. *Environmental and Occupational medicine* 3rd Ed Philadelphia Lippincott Williams & Wilkins 10571064 Chapt 75
17. Sivulka DJ. Assessment of respiratory carcinogenicity associated with exposure to metallic nickel: A review. *Regul Toxicol Pharmacol* 2005;43(2):117–133. [PubMed: 16129532]
18. Oberdorster G, Oberdorster E, Oberdorster J. Nanotoxicology: An Emerging, Discipline Evolving from Studies of Ultrafine Particles. *Environ Health Perspect* 2005;113(7):823–839. [PubMed: 16002369]
19. Donaldson K, Stone V, Clouter A, Renwick L, MacNee W. Ultrafine particles. *Occup Environ Med* 2001;58(3):211–216. [PubMed: 11171936]
20. Nel A, Xia T, Madler L, Li N. Toxic potential of materials at the nanolevel. *Science* 2006;311:622–627. [PubMed: 16456071]
21. Lam CW, James JT, McCluskey R, Hunter RL. Pulmonary toxicity of single-wall carbon nanotubes in mice 7 and 90 days after intratracheal instillation. *Toxicol Sci* 2004;77(1):126–134. [PubMed: 14514958]
22. Lam CW, James JT, McCluskey R, Arepalli S, Hunter RL. A review of carbon nanotube toxicity and assessment of potential occupational and environmental health risks. *Crit Rev Toxicol* 2006;36(3):189–217. [PubMed: 16686422]
23. Warheit DB, Laurence BR, Reed KL, Roach DH, Reynolds GA, Webb TR. Comparative pulmonary toxicity assessment of single-wall carbon nanotubes in rats. *Toxicol Sci* 2004;77(1):117–125. [PubMed: 14514968]
24. Shvedova AA, Castranova V, Kisin ER, Schwegler-Berry D, Murray AR, Gandelsman VZ, Maynard A, Baron P. Exposure to carbon nanotube material: Assessment of nanotube cytotoxicity using human keratinocyte cells. *J Toxicol Environ Health A* 2003;66(20):1909–1926. [PubMed: 14514433]
25. Muller J, Huaux F, Lison D. Respiratory toxicity of carbon nanotubes: how worried should we be? *Carbon* 2006;44(6):1048–1056.
26. Hurt RH, Monthieux M, Kane AB. Toxicology of carbon nanomaterials: status, trends, and perspectives on the special issue. *Carbon* 2006;44(6):1028–1033.
27. Pulskamp K, Diabate S, Krug HF. Carbon nanotubes show no sign of acute toxicity but induce intracellular reactive oxygen species in dependence on contaminants. *Toxicol Lett* 2007;168(1):58–74. [PubMed: 17141434]
28. Kagan VE, Tyurina YY, Tyurin VA, Konduru NV, Potapovich AI, Osipov AN, et al. Direct and indirect effects of single walled carbon nanotubes on RAW 2647 macrophages: Role of iron. *Toxicol Lett* 2006;165(1):88–100. [PubMed: 16527436]
29. Borm P, Klaessig FC, Landry TD, Moudgil B, Pauluhn J, Thomas K, Trottier R, Wood S. Research strategies for safety evaluation of nanomaterials, Part V: Role of dissolution in biological fate and effects of nanoscale particles. *Toxicol Sci* 2006;90:23–32. [PubMed: 16396841]
30. Ghio AJ, Cohen MD. Disruption of iron homeostasis as a mechanism of biologic effect by ambient air pollution particles. *Inhal Toxicol* 2005;17(13):709–716. [PubMed: 16195206]
31. Itkis ME, Perea DE, Niyogi S, Rickard SM, Hamon MA, Hu H, et al. Purity evaluation of as-prepared single-walled carbon nanotube soot by use of solution-phase near-IR spectroscopy. *Nano Lett* 2003;3(3):309–314.
32. Stefaniak AB, Guilmette RA, Day GA, Hoover MD, Breyse PN, Scripsick RC. Characterization of phagolysosomal simulant fluid for study of beryllium aerosol particle dissolution. *Toxicol In Vitro* 2005;19(1):123–134. [PubMed: 15582363]
33. Lambeth JD. NOX enzymes and the biology of reactive oxygen. *Nat Rev Immunol* 2004;4(3):181–189. [PubMed: 15039755]

34. Blackwell JM, Goswami T, Evans CA, Sibthorpe D, Papo N, White JK, Searle S, Miller EN, Peacock CS, Mohammed H, Ibrahim M. SLC11A1(formerly NRAMP1) and disease resistance. *Cell Microbiol* 2001;3(12):773–784. [PubMed: 11736990]
35. Halliwell B, Gutteridge JMC. Role of iron in oxygen radical reactions. *Methods in Enzymol* 1984;105:47–56. [PubMed: 6203010]
36. de Meringo A, Morscheidt C, Thélohan S, Tiesler H. In vitro assessment of biodurability: acellular systems. *Environ Health Perspect* 1994;102:47–53. [PubMed: 7882955]
37. Scholze H, Conradt R. An in-vitro study of the chemical durability of siliceous fibres. *Ann Occup Hyg* 1987;31(4B):683–692.
38. Lay JC, Bennett WD, Ghio AJ, Bromberg PA, Costa DL, Kim CS, et al. Cellular and biochemical response of the human lung after intrapulmonary instillation of ferric oxide particles. *Am J Respir Cell Mol Biol* 1999;20(4):631–642. [PubMed: 10100994]
39. Goodglick LA, Pietras LA, Kane AB. Evaluation of the causal relationship between crocidolite asbestos-induced lipid peroxidation and toxicity to macrophages. *Am Rev Respir Dis* 1989;139(5):1265–1273. [PubMed: 2540689]
40. Konuma, T., et al. Etching material and etching process. US Patent. 5639344. 1997.
41. Hardy JA, Aust AE. Iron in Asbestos chemistry and carcinogenicity. *Chem. Rev* 1995;95:97–118.
42. Lund LG, Aust AE. Iron mobilization from asbestos by chelators and ascorbic acid. *Arch. Biochem. Biophys* 1990;278(1):61–64. [PubMed: 2321970]
43. Snoeyink, VL.; Jenkins, D. *Water Chemistry*. New York: John Wiley & Sons; 1980. p. 382-386.
44. Biniak S, Pakula M, Szymanski GS, Swiatkowski A. Effect of activated carbon surface oxygen- and/or nitrogen-containing groups on adsorption of copper(II) ions from aqueous solution. *Langmuir* 1999;15(18):6117–6122.
45. Johns MM, Marshall WE, Toles CA. Agricultural by-products as granular activated carbons for adsorbing dissolved metals and organics. *J Chem Technol Biotechnol* 1998;71(2):131–140.

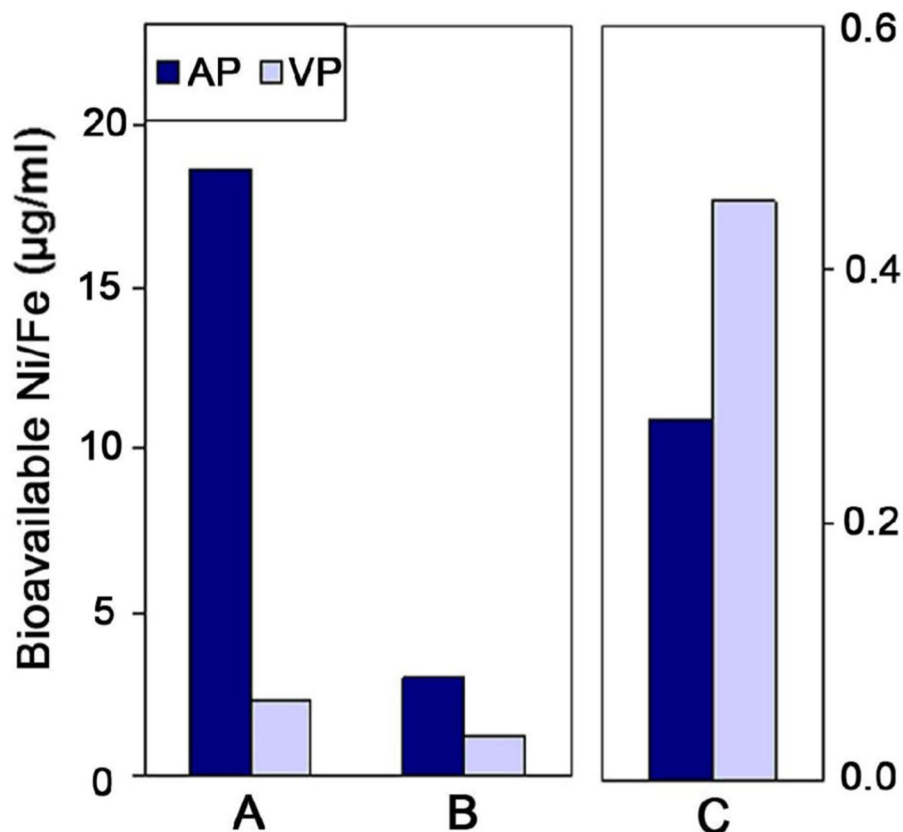


Figure 1. Mobilization (bioavailability) of nickel (A) or iron (B, C) from as-produced (AP) and vendor-purified (VP) single-walled carbon nanotubes (SWCNTs) into simple fluid media [1,2], in which the commercial purification processes leave significant bioavailable metal (A,B) or even increase bioavailable metal (C). Bioavailable Ni from sample A was analyzed by inductively coupled plasma atomic emission spectroscopy (ICP-AES) after incubation in acetate buffer (pH 5.5) for 2 hr. Bioavailable Fe from sample B and C was determined by UV-Vis spectrophotometry after incubation in MOPS aqueous solution at pH 7 with 1 mM ascorbate and ferrozine for 72 hours.

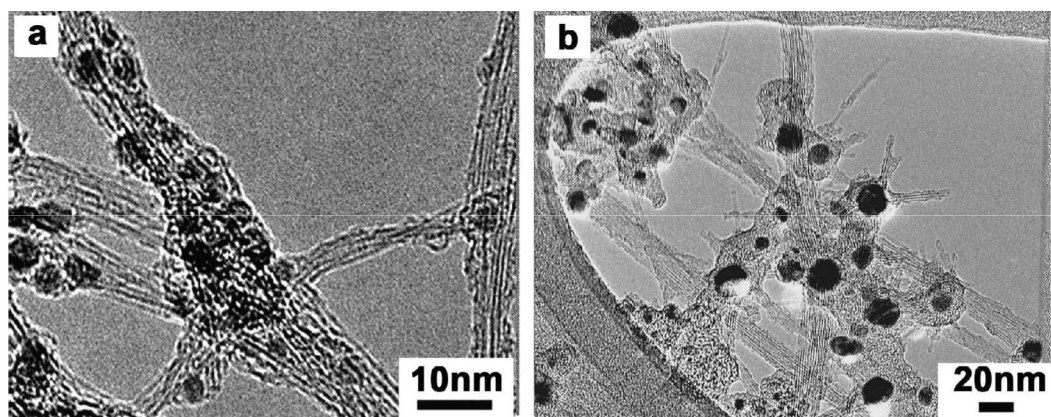


Figure 2. Typical morphologies for metal-containing SWCNTs: (a) Fe-containing as-produced SWCNTs from vendor A (b) Ni-containing AP SWCNTs from vendor C.

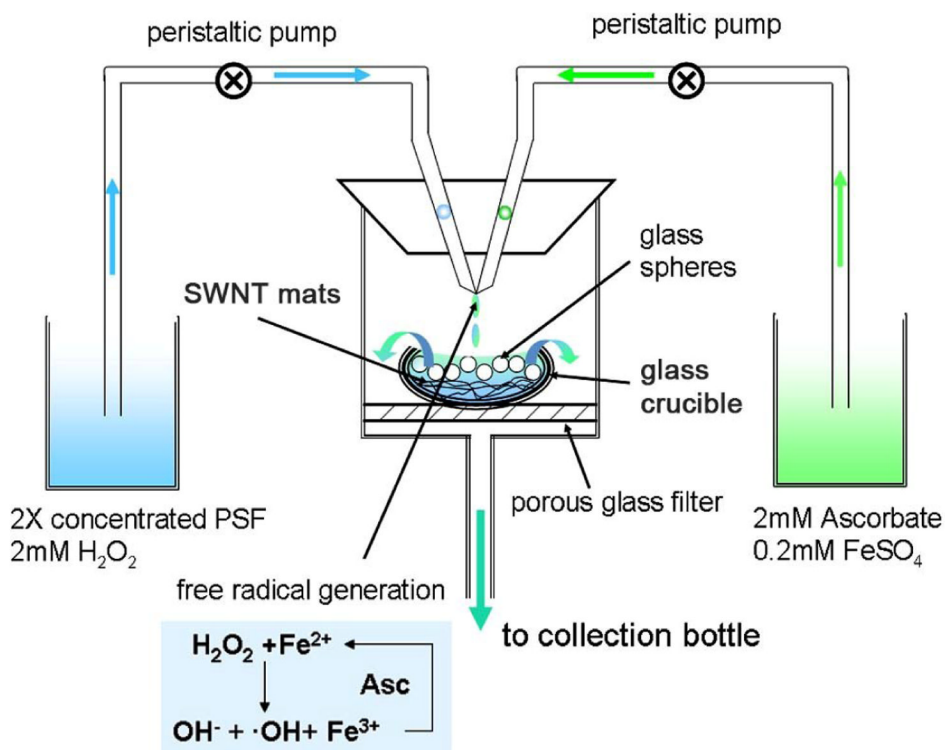


Figure 3. Apparatus for dynamic study of the *in vitro* biopersistence of purified Ni-containing SWCNTs in a simulated phagolysosome with continuous free radical generation.

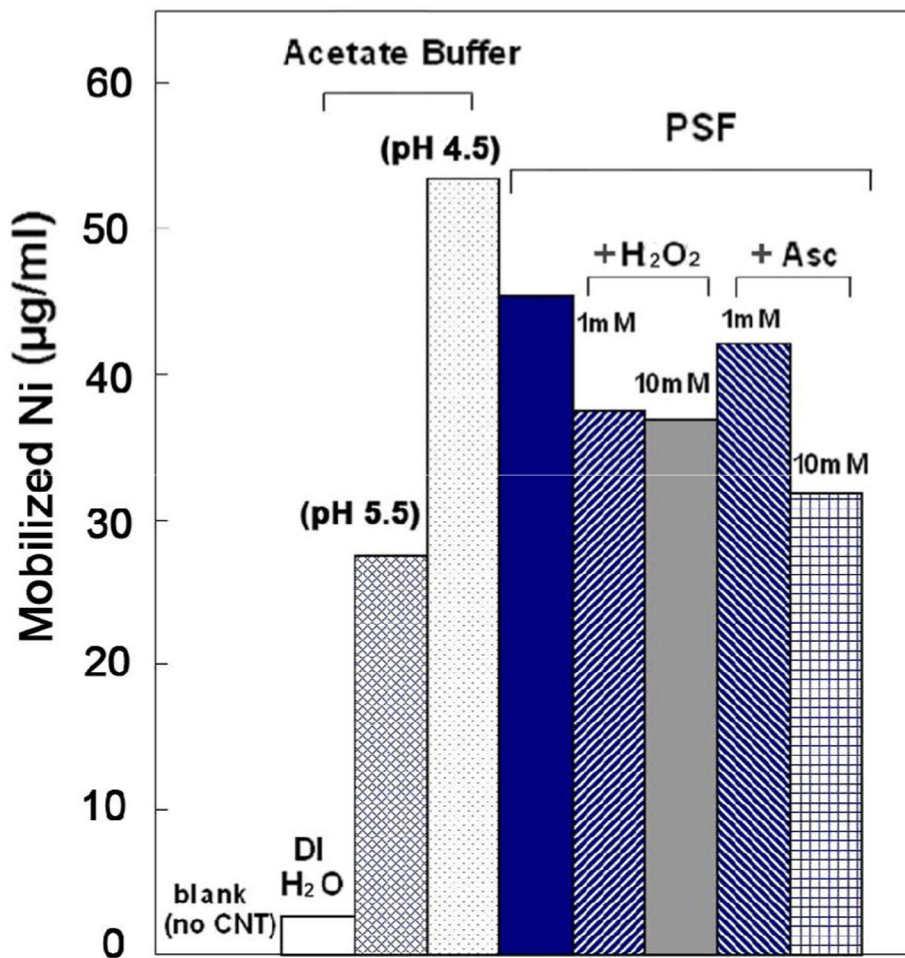


Figure 4. Development of standard nickel bioavailability assay by comparison of Ni mobilization in various aqueous solutions: deionized water (pH 7.0), acetate buffer (pH 5.5 and pH 4.5) and PSF (pH 4.5) for a range of SWCNT samples. Data are for sample C-AP. Additional H₂O₂ or ascorbate (1 or 10mM) did not produce enhanced mobilization by oxidation or reduction.

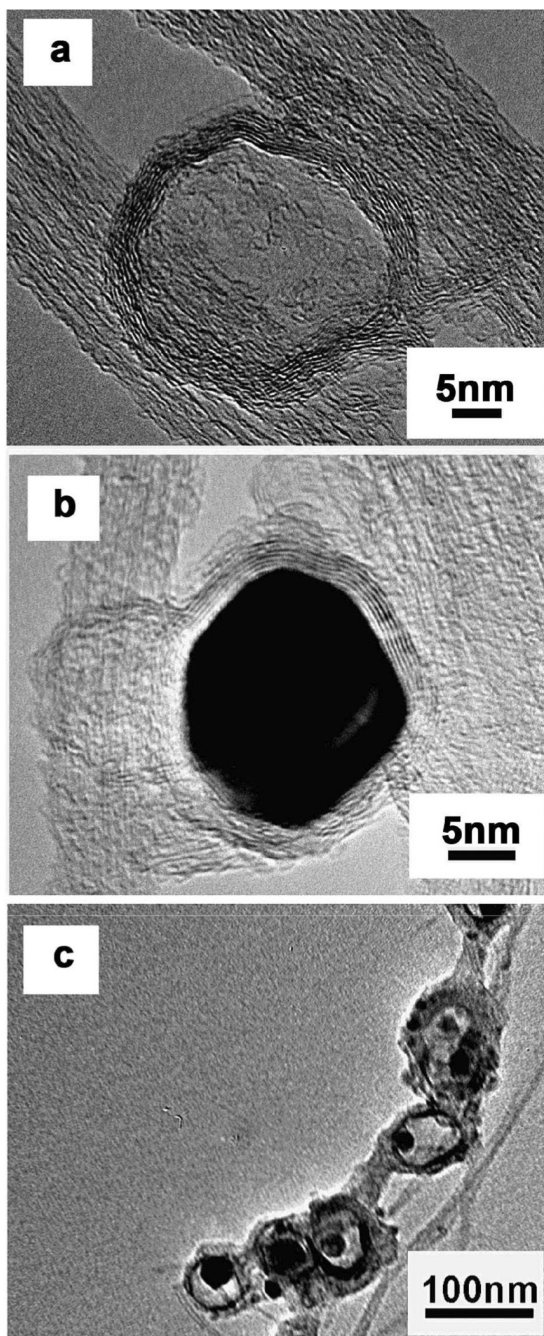


Figure 5.

Evidence for kinetic limitations in acid dissolution during purification. HRTEM images of commercial samples “C” showing a range of observed morphologies following 3M HCl treatment for 48 hrs. The most commonly observed morphologies are (a) empty shells, and (b) shells with intact Ni-containing nanoparticles. This implies the presence of pore-free carbon shells that are fully protective of the imbedded catalyst, and the presence of some defective shells that allow sufficient fluid access to remove Ni. Also seen, however, as minority features (c) are carbon shells with *partially etched* Ni nanoparticles, implying that the acid dissolution process was still underway at the end of the treatment time. These shells likely contain more subtle defects that allow only slow transport of etching reactants and products.

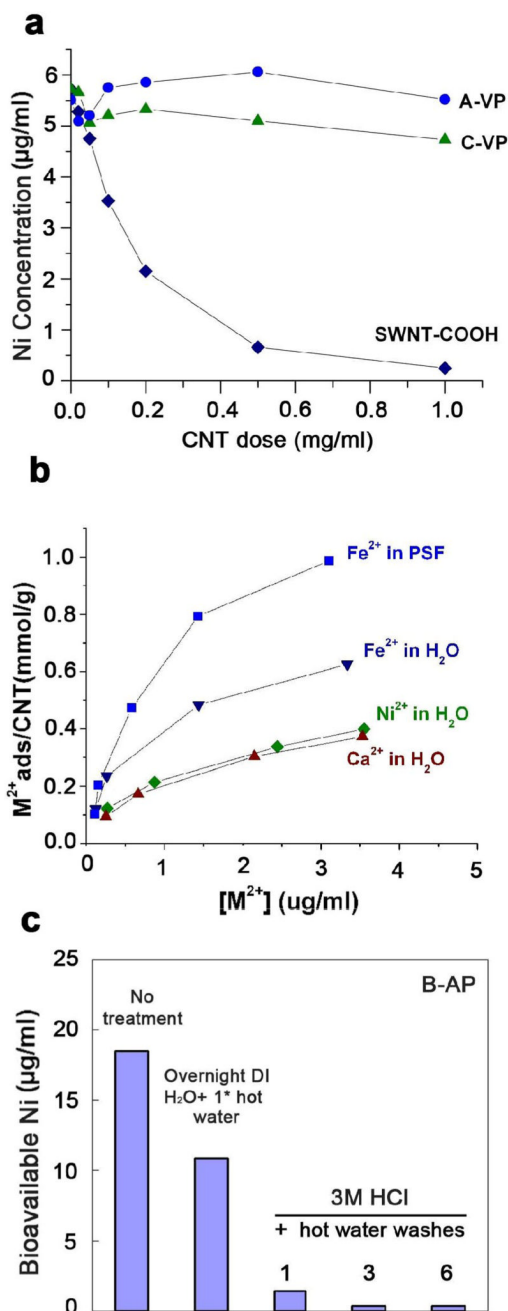


Figure 6. Evidence for the re-deposition of Ni on the free surfaces of nanotubes following acid washing. (a) Active adsorption of soluble Ni onto SWCNTs from standard NiCl₂ solutions, especially pronounced for the COOH-functionalized tubes; (b) equilibrium adsorption isotherms for various cations on COOH-functionalized SWCNTs. This sample has 4–6 atomic-% COOH groups and the amount adsorbed (up to 1 mmol/g) corresponds stoichiometrically to a significant fraction of COOH sites occupied by the cation. The results in (a) and (b) demonstrate the *potential* for re-deposition through adsorption; (c) Evidence that insufficient washing (e.g. 1 wash only) following acid treatment can lead to detectable residual free Ni, presumably by the mechanism of panel (a) and (b).

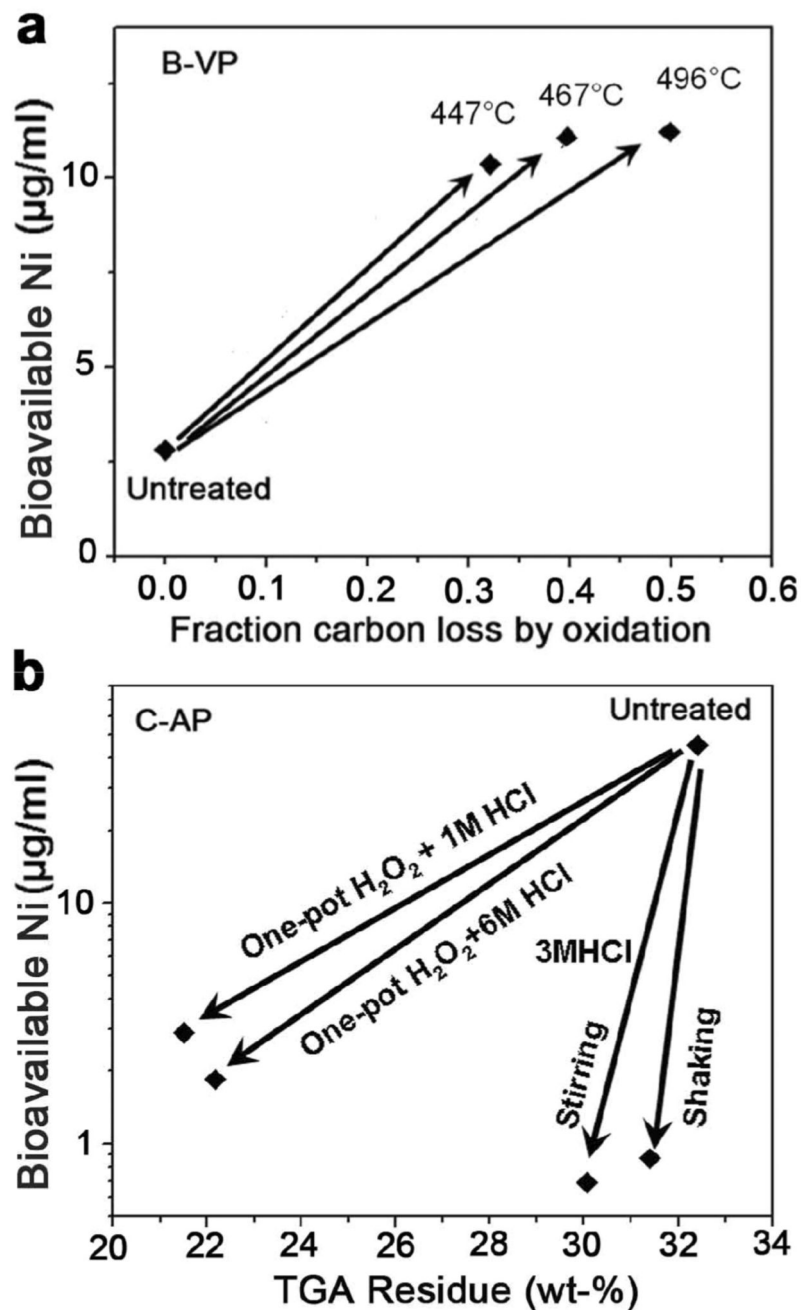


Figure 7. Evidence that oxidation either after (a) or during (b) acid treatment can leave residual bioavailable metal in “purified” CNTs. (a) Effect of air oxidation on Ni bioavailability from a vendor purified sample (B-VP); (b) effect of simultaneous oxidation and acid treatment (one-pot purification process [9]) on Ni bioavailability from sample C-A). The one-pot method removes more total metal (indicated by TGA residue), but leaves higher residual bioavailable metal than simple acid treatment.

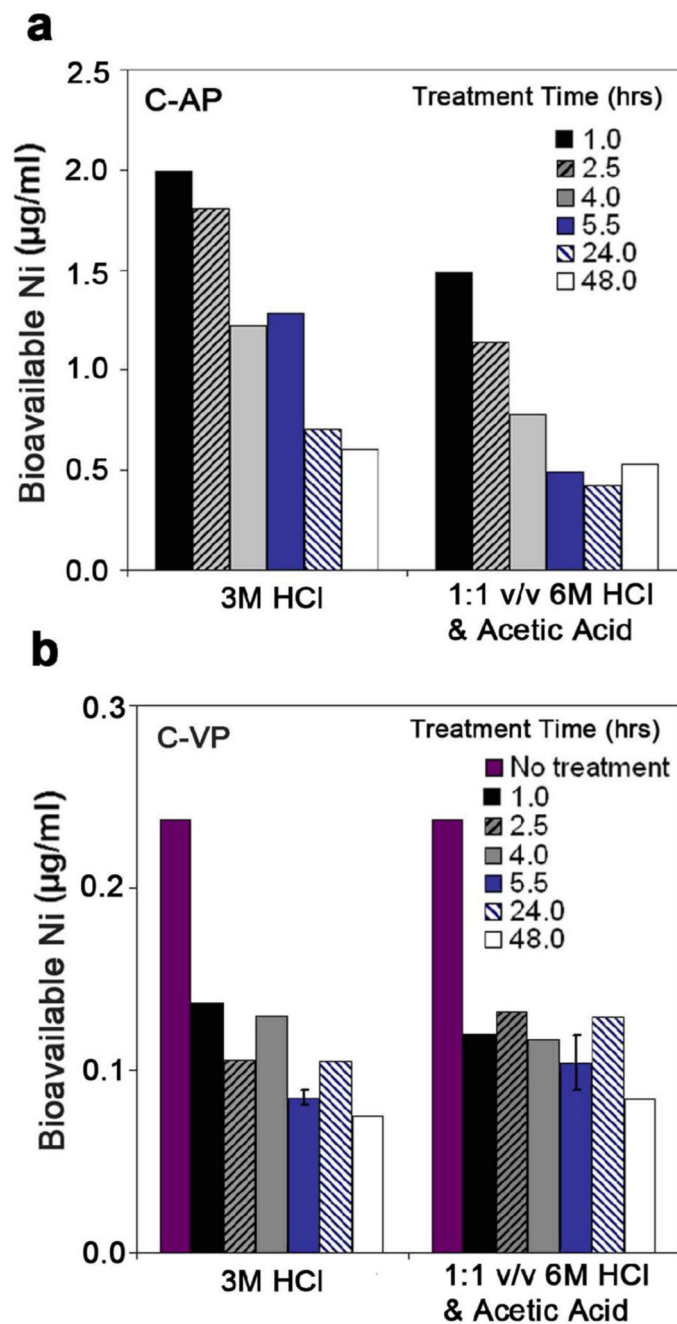


Figure 8. Effect of treatment time on bioavailable Ni removal by 3 M HCl. (a) as-produced SWCNTs, (b) vendor-purified SWCNTs. In each case this acid treatment is followed by three rounds of hot water washing. Bioavailable Ni was mobilized into PSF (pH 4.5) and then analyzed by ICP.

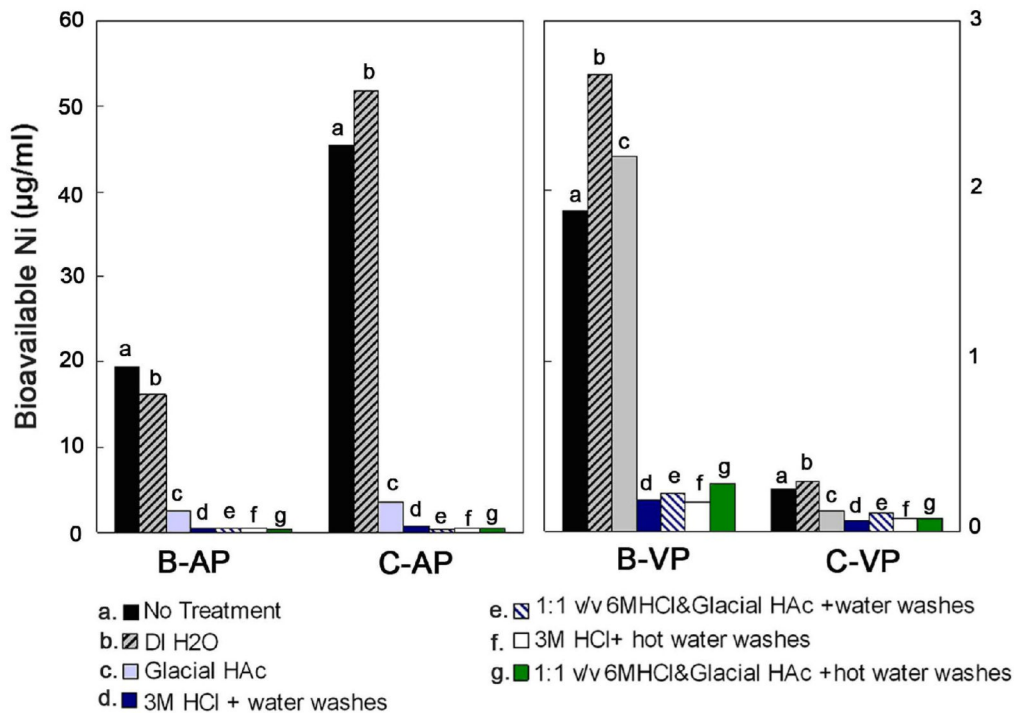


Figure 9. Effect of acid composition and sample origin on targeted removal of bioavailable Ni from SWCNTs (treatment time: 24hr).

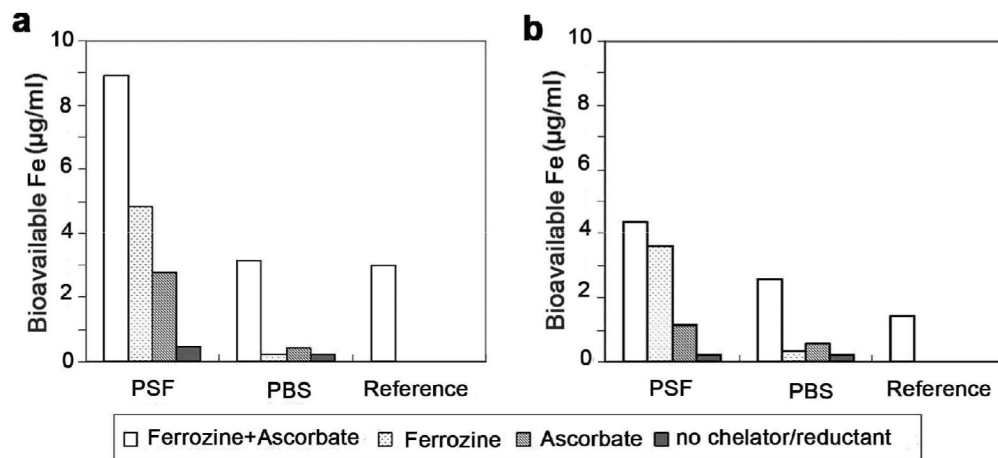


Figure 10.

Comparison of competing media (PSF at pH 4.5 and PBS at pH 7.4) for the measurement of iron bioavailability in CNTs. (a): A-AP, (b): A-VP. “Reference” is data from previous study [1], which measured mobilization optically with ferrozine at pH 7 and 1 mM ascorbate after 72 hours incubation.

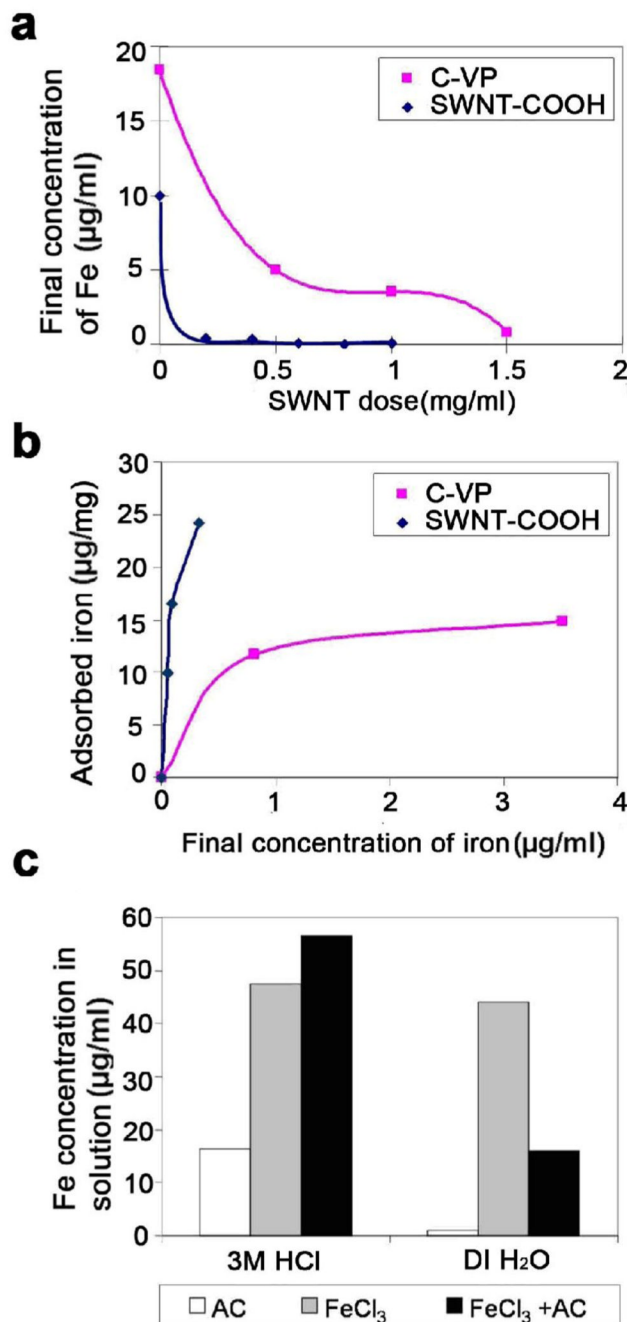


Figure 11.

Evidence that soluble Fe can be adsorbed from solution onto SWCNT surfaces. a) Raw measurements of iron concentration after 24-hr incubation of SWCNTs in a PBS buffer containing FeCl₃; b) Presentation of same data as equilibrium adsorption isotherms; c) Similar experiment for activated carbon as a model, high-surface-area carbon material. In 3M HCl the activated carbon is a net source of soluble iron through release of iron impurities. At neutral pH adsorption dominates and activated carbon is a net sink for soluble iron in a similar manner to SWCNTs.

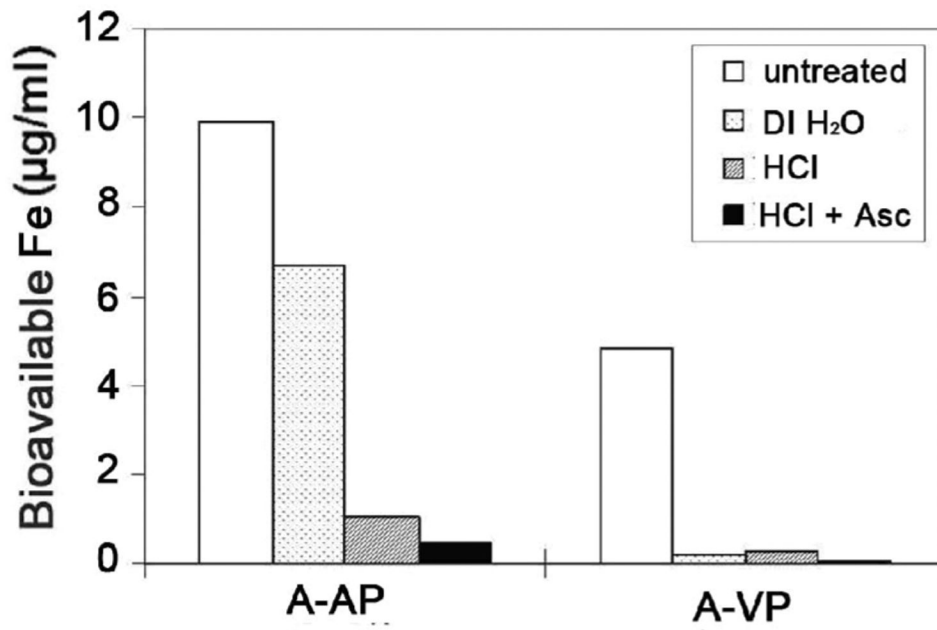


Figure 12. Effects of different acid washing on removal of bioavailable iron for A-AP and A-VP SWCNT samples

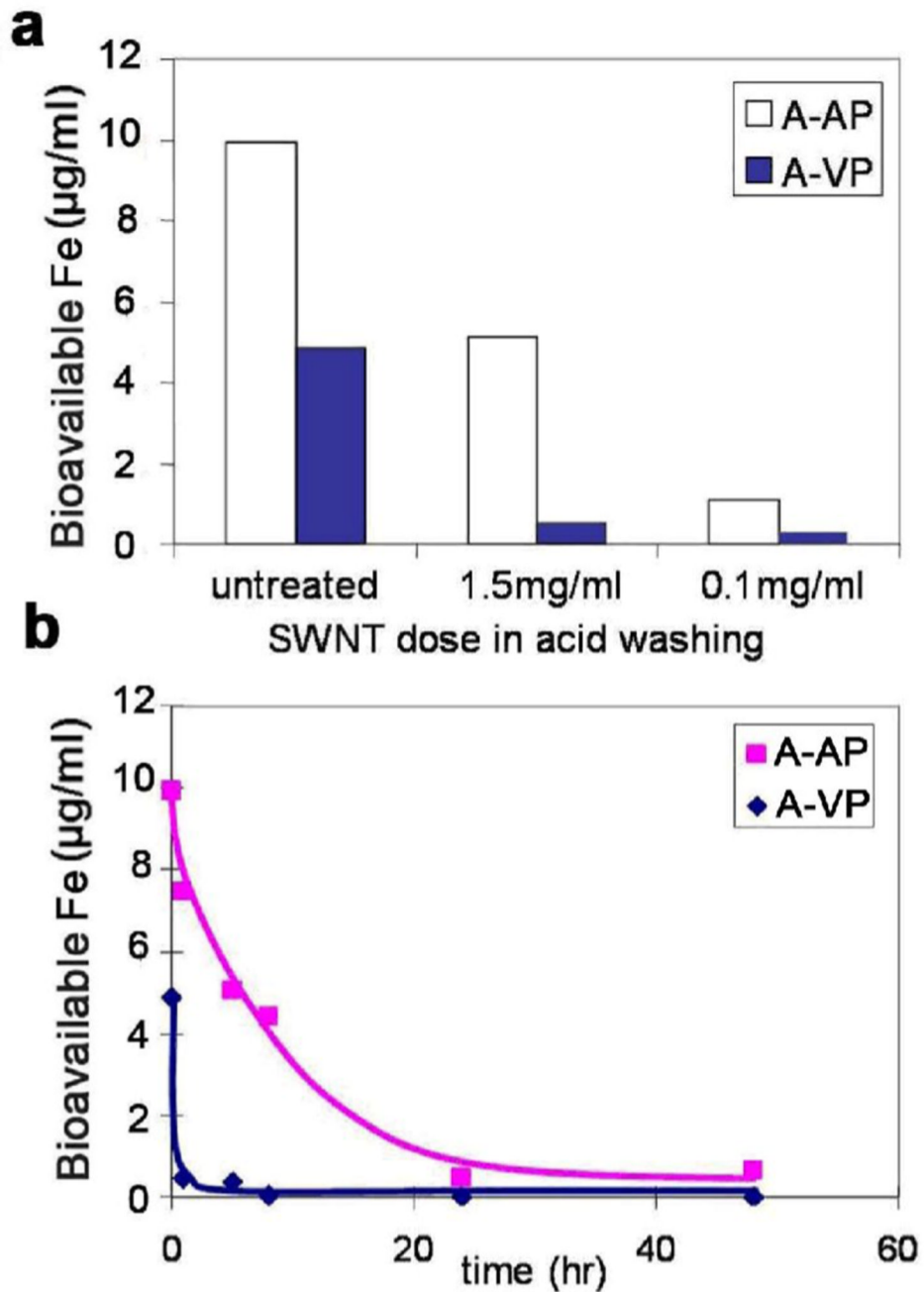


Figure 13. Effects of acid/CNT ratio (a) and time (b) on the removal of bioavailable iron for two SWCNT samples.

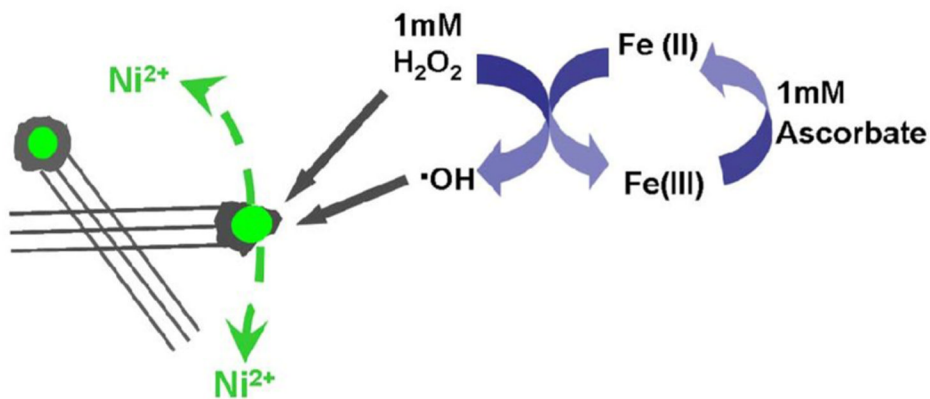


Figure 14.

Potential Ni release mechanism by oxidative attack on carbon shells in phagolysosomes. Wide arrows show oxidant generation in the long-term dynamic flow-through assay developed here. This assay is designed to test the stability of encapsulated metal using a flowing PSF simulant (pH 4.5) supplemented with ascorbate, H_2O_2 , and Fe^{2+} for continuous generation of reactive oxygen species.

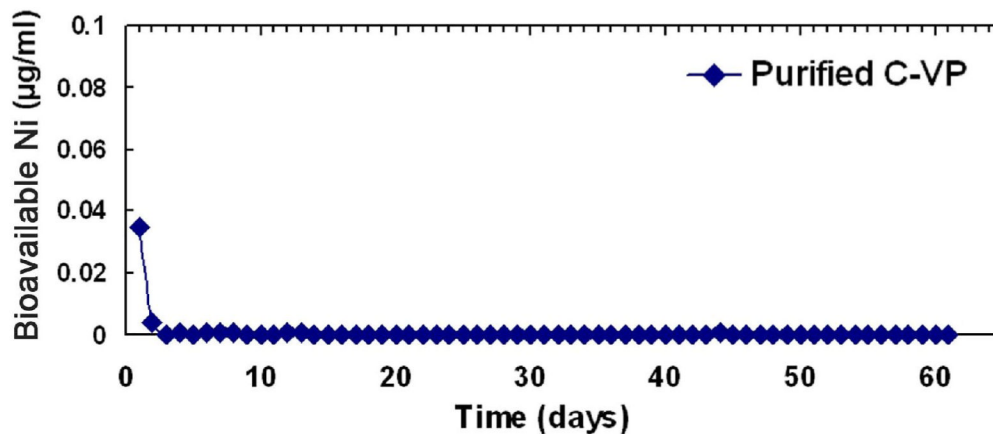


Figure 15.

Results of flow-through assay to assess the stability of non-bioavailable (encapsulated) Ni remaining after optimized acid treatment of a commercial SWCNT sample. Y-axis gives the total Ni content of the effluent. The assay uses a phagolysosomal simulant augmented for continuous generation of reactive oxygen species. Following the initial release of a trace amount of Ni, there is no detectable release and thus no indication of significant oxidative attack on the covering carbon shells for two months.

Table 1

Total metals content determined by inductively coupled plasma atomic emission spectroscopy (ICP) for the six* commercial SWCNT samples used in this study

Sample	Vendor Specification	Metal content by ICP
A-AP	Fe 26%	Fe 22.2%, Ni 0.016%, Co 0.003%
A-VP	Fe 10%	Fe 10.9%, Ni 0.028%, Co 0.026%
B-AP	Carbonaceous purity** 40–60% Metal content 30%	Ni 19.4%, Y 5.49%, Fe 0.041%, Co 0.010%, Mo<0.002%
B-VP	Carbonaceous purity 60–80% Metal content 15%	Ni 14.28%, Y 2.09%, Fe 0.050%, Co<0.002%, Mo 0.060%
C-AP	Carbonaceous purity 40–60% Metal content 30%	Ni 23.3%, Y 5.77% Fe 0.032%, Co 0.0014%, Mo<0.0001%
C-VP	Carbonaceous purity 70–90% Metal content 7–10%	Ni 6.70%, Y 1.30%, Fe 0.017%, Co 0.0002%, Mo 0.0006%

* Selected experiments used a seventh sample: commercial COOH-functionalized SWCNTs which were reported to have 80–90% carbonaceous purity and 5–10% metal content.

** Carbonaceous purity is defined in the literature as the mass ratio of pure SWCNT to the total carbonaceous material and it is evaluated by near-IR spectroscopy against a reference sample [31].

Table 2

Chemical compositions of phagolysosomal simulant fluid using 0.02 M potassium hydrogen phthalate buffer*

Constituent	Concentration (mg/L)
Na ₂ HPO ₄	142.0
NaCl	6650.0
Na ₂ SO ₄	71.0
CaCl ₂ ·2H ₂ O	29.0
Glycine (C ₂ H ₅ NO ₂)	450.0
Potassium hydrogen phthalate (1-(HO ₂ C)-2-(CO ₂ K)-C ₆ H ₄)	4084.6
Alkylbenzyltrimethylammonium chloride**	50ppm

* Our experiments use pH 4.5, obtained by adjusting the original 4.0 pH using 0.1-M potassium hydroxide.

** serves as an anti-fungal agent.